Available online at www.sciencedirect.com
ScienceDirect
Journal of Molecular Catalysis A: Chemical 265 (2007) 258–267
JOURNAL OF MOLECULAR CATALYSIS A: CHEMICAL
www.elsevier.com/locate/molcata

Synthesis, characteristics and catalytic activity of water-soluble [Pd(lysine·HCl)$(Cl)_2$] complex as hydrogenation catalyst

Yu-Zhi Hao [a,b,*], Zuo-Xi Li [a], Jin-Lei Tian [a]

[a] *Department of Chemistry, Nankai University, Tianjin 300071, PR China*
[b] *School of Chemical Engineering, Hebei University of Technology, Tianjin 300130, PR China*

Received 13 November 2005; received in revised form 19 December 2005; accepted 28 September 2006
Available online 6 October 2006

Abstract

Two water-soluble Pd–aminoacid complexes were prepared under mild condition and were characterized by various techniques such as IR, UV–vis, ^{1}H NMR spectra. X-ray crystallography reveals the structure of Pd–valine complex with the molecular formula of [Pd(valine)$_2$]·H_2O and the composition of Pd–lysine complex was suggested as [Pd(lysine·HCl)$(Cl)_2$] at pH 2–5.5. Hydrogenation performance of Pd–lysine complex in two-phase was evaluated by using *p*-chloronitrobenzene. The hydrogenation and dimer performance of Pd–lysine complex was also evaluated by using 2-nitro-5-chlorobenzotrifluride.

Keywords: Pd–lysine; Hydrogenation; Water-soluble; Two-phase; Catalyst

1. Introduction

Two-phase catalysis with water-soluble catalysts offers the most important principle for catalyst recycling in homogeneous catalysis [1–3]. Water-soluble catalyst plays an important key for the catalyst separation, because the product can thus easily be obtained by simple phase separation. The special issues about catalysis in water have been given [4–7]. The water-soluble catalysts are mainly the complex catalyst with the water-soluble ligands [6–11]. The structures of these ligands are various, so the catalytic activities of their complexes are also different. The water-soluble palladium acetate/triethoxylsilane catalysts for alkene and alkyne hydrogenation have been researched [12,13]. Pd–di(sodium alizarinmonosulfonate) as catalyst of unsaturated fatty acids etherified in liquid has been developed [14]. Polyaminodiphosphine dendrimer was used as support for rhodium and palladium catalyst [15]. Palladium/TPPTS or BINAS (BINAS = mixture of tetra-, penta-, hexa-sulfonated 2,2′-bisdiphenylphosphinomethylene binaphthyl) was used as catalyst of aromatic nitro compounds ($ArNO_2$) hydrogenation under CO (2–8 atm) and 80 °C [16]. Tafesh and Beller [8] employed palladium complexes involving water-soluble ligands such as TPPTS or BINAS for reduction of various aromatic nitro compounds under CO (60–120 bar) and H_2O condition. The nitro group was reduced selectively to an amine whereby other functional groups, *i.e.* ketone, nitrile, chloride and alkene were not influenced. Though the catalytic activities and selectivities of these catalysts are high enough, the synthesis of these ligands is difficult, so cheaper water-soluble ligands are expected.

Lysine is a kind of water-soluble ligand and very cheap, but how to prepare the complex with catalytic activity between lysine and Pd is the key. Preparation of water-soluble Pd–aminoacid complex was discussed in this paper. The complexes were characterized by IR, UV–vis, ^{1}H NMR spectra and single crystal diffraction techniques. The synthesis condition, composition and structure of Pd–lysine complex with catalytic activity were discussed. Hydrogenation performance of Pd–lysine complex in two-phase was evaluated by using *p*-chloronitrobenzene to give *p*-chloroaniline. The hydrogenation and dimerization of 2-nitro-5-chlorobenzotrifluride was evaluated, too.

* Corresponding author at: School of Chemical Engineering, Hebei University of Technology, Tianjin 300130, PR China. Tel.: +86 22 60204303; fax: +86 22 60204019.
E-mail address: hyzhsong@sina.com (Y.-Z. Hao).

1381-1169/$ – see front matter © 2006 Elsevier B.V. All rights reserved.
doi:10.1016/j.molcata.2006.09.045

2. Experimental

2.1. Material

Lysine·HCl and valine were obtained from Tianjin reagent company. Pd metal was from Chinese Jinchuan colored metal company. The *p*-chloronitrobenzene (99%) and 2-nitro-5-chlorobenzotrifluride (97%) were obtained commercially and were used directly.

2.2. Preparation of the water-soluble Pd–aminoacid complex

H_2PdCl_4 solution was prepared by adding 2.1093 g commercial palladium metal (99.99%) and 20 mL HCl (33%) in 100 mL three-necked flask with water bath, then stirring and slowly dropping 10 mL H_2O_2 solution (30%), controlling the mixture temperature below 30 °C until all palladium metal dissolved, finally diluting the solution to 100 mL.

The preparation of Pd–lysine complex was shown as follows: 10.0 mL the H_2PdCl_4 (21.09 mg/mL) solution prepared above was diluted to 30 mL in a 100 mL three-necked flask, the pH was adjusted to 3–6 by dropping 0.1 mol/L NaOH solution, then 0.3641 g (1.995 mmol) lysine·HCl was added. The mixture was stirred at 60–70 °C for 2 h.

The Pd–valine complex was prepared by the same procedure (the valine was 1.995 mmol).

The single crystal of Pd–valine was prepared by adding the 10 mL solution of Pd–valine complex in a test-tube and was allowed to stand at room temperature. After about 2 weeks, yellow well-shaped prismatic crystals were obtained at the bottom of test-tube, and many of them were suitable for X-ray diffraction studies.

2.3. Two-phase hydrogenation reaction in the autoclave

All reactions were carried out in 1 L stainless pressure vessel.

2.3.1. Hydrogenation reaction

Hundred millilitres of *p*-chloronitrobenzene and 80 mL deionised water were added into the autoclave, the pH of the mixture was adjusted to about 6 by acetic acid, then 35 mL Pd–lysine complex was poured. The autoclave was pressed and vented three times with N_2 and H_2, respectively, and the pressure was set to 0.1–0.4 MPa. The autoclave was heated to 40 °C and the reaction commenced by starting the stirring. After 4 h, the autoclave was cooled to room temperature, depressurized and replaced three times by N_2. The organic phase was separated and immediately analyzed with GC. The water phase can be recycled.

2.3.2. Hydrogenation and dimerization reaction

Hundred millilitres of 2-nitro-5-chlorotrifluoride and 80 mL ethanol were added into autoclave, then 5 mL acetic acid, finally 35 mL Pd–lysine complex was poured. The autoclave was pressed and vented three times with N_2 and H_2, respectively, and the pressure was set to 0.4 MPa. The autoclave was heated to 40 °C and the reaction commenced by starting the stirring. After 4 h, the autoclave was cooled to room temperature, depressurized and replaced three times by N_2. The reaction product was sheet and light yellow crystal. The elemental analysis of the product was C 40.45%; N 7.17%; H 2.15%; Cl 18.69%. The crystal was dissolved in $CHCl_3$ and analyzed with GC–MS.

2.4. Sample characterization

UV–vis spectra were recorded on HITACHI UV-3010 spectrometer. ^{1}H NMR spectra were carried out on a Varian Mercury V × 300 spectrometer in D_2O, TMS was used as standard for ^{1}H NMR spectra. Elemental analysis was performed on an Elementar Vario EL system. IR spectra were taken on a Bruker TENSOR 27 spectrometer.

The reaction product was analyzed on Shimadzu GC-9A gas chromatograph with polyglycol capillary column (30 m) and FID detector, and on MASPEC II GC–MS system.

X-ray structure determination of Pd–valine was carried out on a Bruker Smart 1000 CCD diffractometer equipped with a graphite crystal monochromator situated in the incident beam for data collection at 293(2) K. The determinations of unit cell parameters and data collections were performed with Mo Kα radiation (λ = 0.71073 Å) and unit cell dimensions were obtained with least-squares refinements. The program SAINT [17] was used for integration of the diffraction profiles. The structure was solved by direct methods using the SHELXS program of the SHELXTL package and refined with SHELXL [18]. All non-hydrogen atoms were located in successive difference Fourier syntheses. The final refinement was performed by full matrix least-squares methods with anisotropic thermal parameters for non-hydrogen atoms on F^2. The hydrogen atoms were added theoretically, riding on the concerned atoms and refined with fixed thermal factors.

3. Results and discussion

3.1. Preparation of Pd–lysine complex

Three millilitres 0.1 mol/L NaoH solution and 6.9 mg (0.038 mmol) lysine·HCl were added in 5.0 mL H_2PdCl_4 solution (Pd 0.81 mg/mL), the mixture was stirred at room temperature, the UV–vis spectra of the mixture were recorded as the reaction time increased (Figs. 1 and 2).

From the UV–vis spectra, the maximum Abs of UV–vis spectra shifted from about 428 nm to 392 nm as the reaction time increased and became stable after about 120 min, therefore a new complex was formed after H_2PdCl_4 solution reacted with lysine·HCl.

In the same way, the relation between maximum Abs of UV–vis spectra and reaction time of the mixture at 50 °C was summarized in Fig. 3. Similarly, the maximum Abs of UV–vis spectra shifted from about 428 nm to 392 nm as the reaction time increased and became stable after about 33 min, therefore the complex reaction was the same at different reaction temperature, and the rate of complex reaction became faster as the reaction temperature raised.

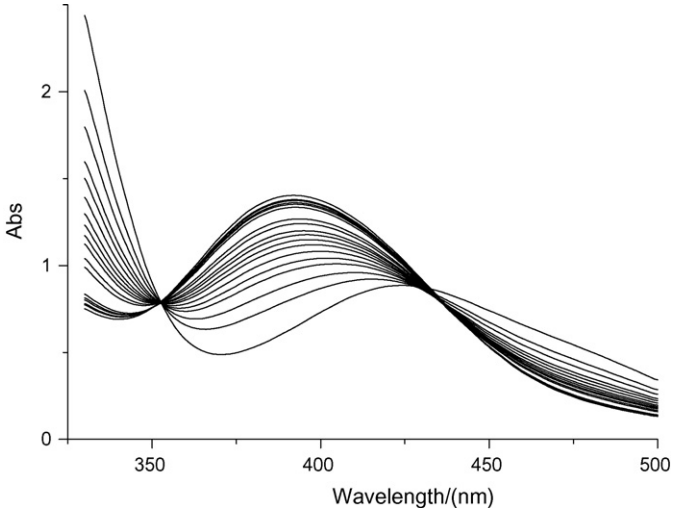

Fig. 1. The UV–vis spectra of Pd–lysine complex as reaction time at room temperature.

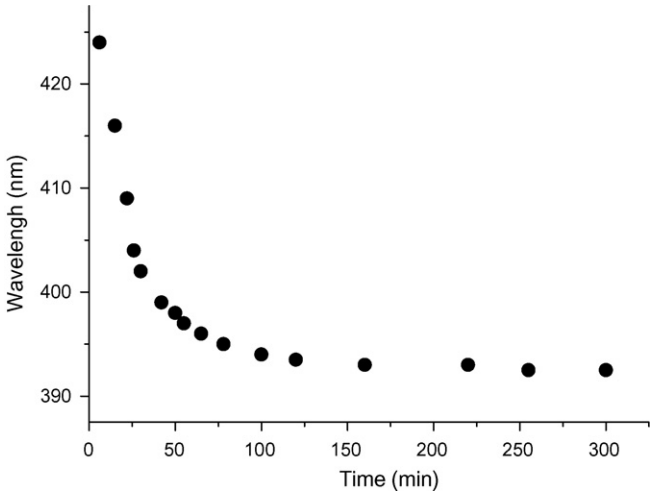

Fig. 2. The maximum Abs of UV–vis spectra of Pd–lysine complex as reaction time at room temperature.

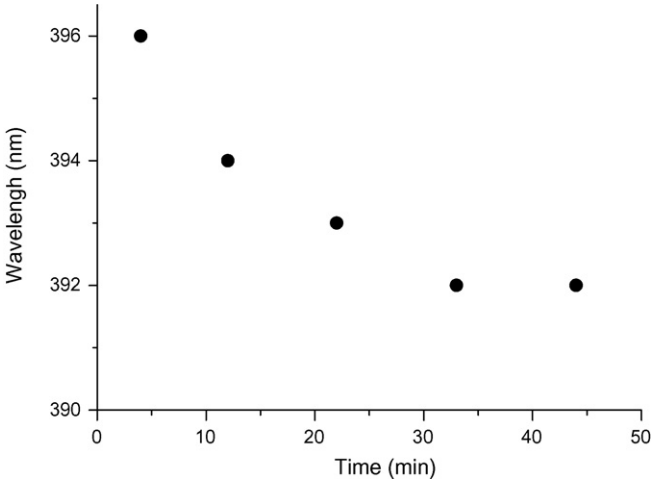

Fig. 3. The maximum Abs of UV–vis spectra of Pd–lysine complex as reaction time at 50 °C.

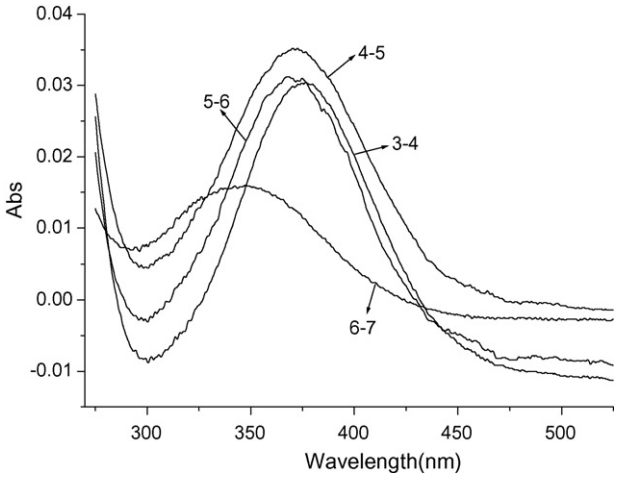

Fig. 4. The UV–vis spectra of Pd–lysine complexes prepared at different pH.

The Pd–lysine mixtures were prepared at different pH by NaOH solution adjusting. The UV–vis spectra of these mixtures after reaction at 70 °C for 1 h were recorded in Fig. 4. Obviously, the UV–vis spectra of Pd–lysine complexes were similar between pH 3 and 6, so the Pd–lysine complex prepared was stable at pH 3–6. But when pH was above 6, the UV–vis spectrum changed obviously, the maximum Abs shifted from about 392 nm to 340 nm, therefore the complex structure was different from that of at pH 3–6.

Thus according to these results, the Pd–lysine complex may be prepared at 50–70 °C for 1 h and stable at pH 3–6.

3.2. The structure of Pd–lysine complex

3.2.1. The coordinate ratio of metal:ligand of Pd–lysine complex

Eighteen millilitres 0.1 mol/L NaOH solution was added into 30 mL H_2PdCl_4 solution (Pd 0.81 mg/mL), the pH of mixture was about 4. The mixture was stirred and heated to 60 °C for 1 h, then 8.3 mg lysine·HCl was poured, the UV–vis spectrum of the mixture was examined after reaction for 30 min. In the same way, each adding 8.3 mg lysine·HCl in the mixture, the UV–vis spectrum of the mixture was recorded after reaction for 30 min, the mole ratio of n(lysine·HCl)/n(H_2PdCl_4) was separately 0.20, 0.39, 0.60, 0.79, 0.98, 1.18, 1.38, 1.57, 1.77, 1.97, 2.16, 2.36, 2.56, 2.75, 2.95, 3.15, 3.34, 3.54. The corresponding curves were nos. 1–18. After the sixth adding, the UV–vis spectra of the mixture became similar (from Fig. 5). So when the mole ratio of n(lysine·HCl)/n(H_2PdCl_4) was about 1.18, the complex did not changed. After the sixth adding, the lysine·HCl did not react again with any substance. According to the curve of between UV–vis Abs and the mole ratio of n(lysine·HCl)/n(H_2PdCl_4) at pH 4 (Fig. 6), the inflexion of the curve was at the mole ratio of n(lysine·HCl)/n(H_2PdCl_4) = 1.00, so the complex between lysine·HCl and Pd prepared at pH 4 was 1:1 (metal:ligand) complex.

Thirty millilitres of H_2PdCl_4 solution (Pd 0.81 mg/mL), the pH of solution was about 2, was heated to 70 °C for 1 h, then 8.3 mg lysine·HCl was added. The UV–vis spectrum of the mix-

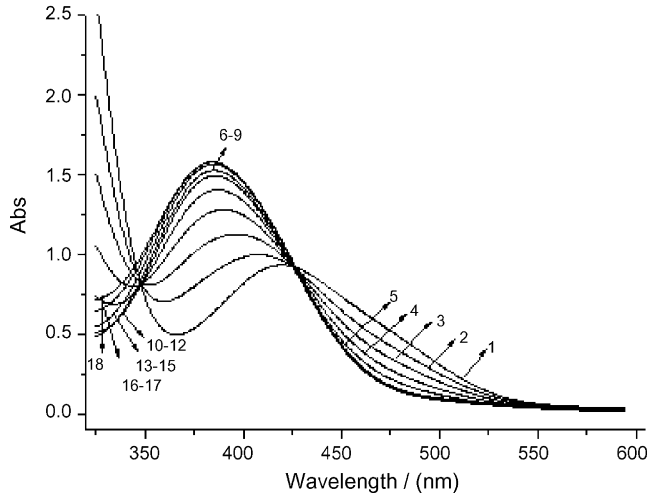

Fig. 5. The UV–vis spectra of Pd–lysine complex at different mole ratio of n(lysine·HCl)/n(H_2PdCl_4) at pH 4.

ture was examined after 30 min. In the same way, each adding 8.3 mg lysine·HCl in the mixture, the UV–vis spectrum of the mixture was recorded after reaction for 30 min, the mole ratio of n(lysine·HCl)/n(H_2PdCl_4) was separately 0.20, 0.39, 0.60, 0.79, 0.98, 1.18, 1.38, 1.57, 1.77, 1.97, 2.16, 2.36, 2.56. The corresponding curves were nos. 1–13. After each adding, the UV–vis spectra of the mixture were different (from Fig. 7). According to the curve of between UV–vis Abs and the mole ratio of n(lysine·HCl)/n(H_2PdCl_4) at pH 2 (Fig. 8), the inflexion of the curve was at the mole ratio of n(lysine·HCl)/n(H_2PdCl_4) = 0.99, but after the fifth adding, the UV–vis Abs continue to rise, the coordination structure has not stopped changing, so the complex between lysine·HCl and Pd prepared at pH 2 was not 1:1 (metal:ligand) complex.

A 21.6 mL 0.1 mol NaOH solution was added into 30 mL H_2PdCl_4 solution (Pd 0.81 mg/mL), the pH of mixture was about 5.5. By the same method above, the UV–vis spectrum of the mixture was recorded (Fig. 9). After each adding

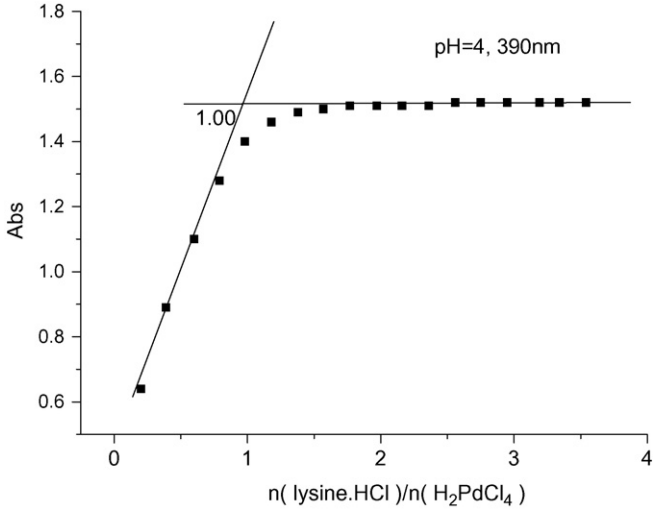

Fig. 6. The curve between UV–vis Abs and the mole ratio of n(lysine·HCl)/n(H_2PdCl_4) at pH 4.

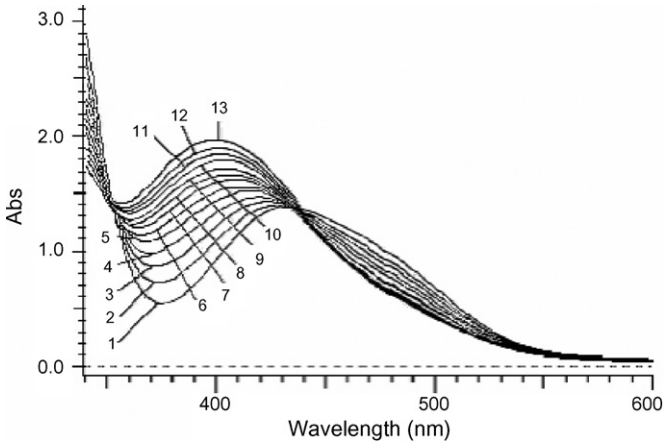

Fig. 7. The UV–vis spectra of Pd–lysine complex at different mole ratio of n(lysine·HCl)/n(H_2PdCl_4) at pH 2.

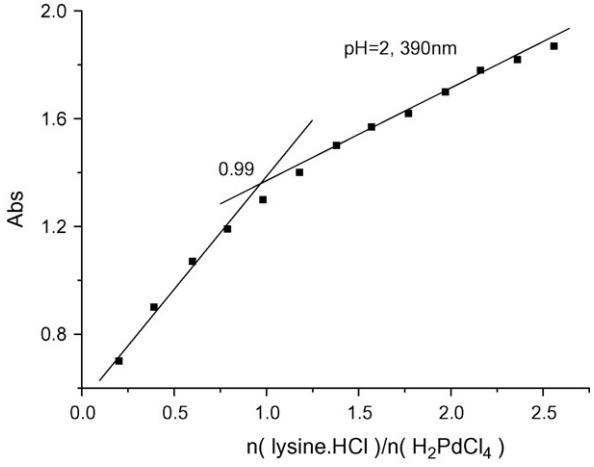

Fig. 8. The curve between UV–vis Abs and the mole ratio of n(lysine·HCl)/n(H_2PdCl_4) at pH 2.

lysine·HCl, the UV–vis spectra of the mixture were different. According to the curve of between UV–vis Abs and the mole ratio of n(lysine·HCl)/n(H_2PdCl_4) at pH 5.5 (Fig. 10), the inflexion of the curve was at the mole ratio of

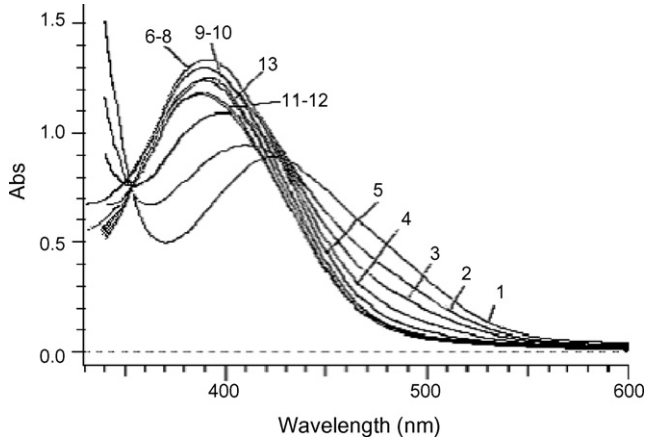

Fig. 9. The UV–vis spectra of Pd–lysine complex at different mole ratio of n(lysine·HCl)/n(H_2PdCl_4) at pH 5.5.

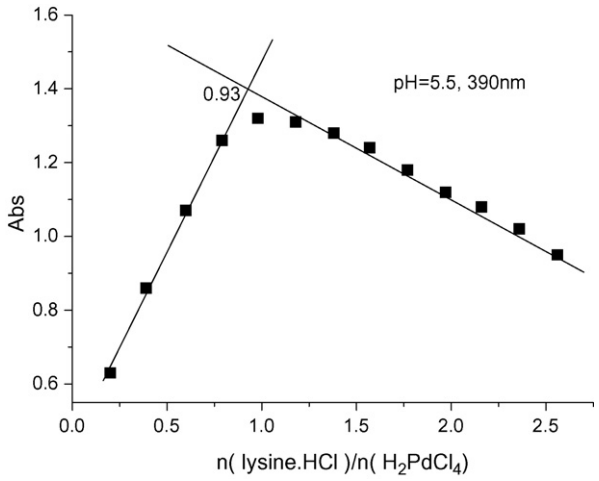

Fig. 10. The curve between UV–vis Abs and the mole ratio of n(lysine·HCl)/n(H_2PdCl_4) at pH 5.5.

n(lysine·HCl)/n(H_2PdCl_4) = 0.93, but after the fifth adding, a few deposits appeared, the UV–vis Abs became to fall, so the complex between lysine·HCl and Pd prepared at pH 5.5 was not 1:1 (metal:ligand) complex, too.

Therefore, only pH of the mixture was at between 2 and 5.5, the complex between lysine·HCl and Pd prepared was 1:1 (metal:ligand) complex, the composition of Pd–lysine complex was [Pd(lysine·HCl)$(Cl)_2$]. When pH was above 5.5 or under 2, the coordinate ratio of complex between lysine·HCl and Pd was uncertain, thus the complex was not suitable to catalyst.

3.2.2. The coordinate structure of the Pd–lysine complex

The UV–vis spectra of lysine·HCl, valine, Pd–lysine complex, Pd–valine complex and H_2PdCl_4 solution were summarized in Fig. 11. Obviously, UV–vis Abs of H_2PdCl_4 solution (428 nm) was different from those of Pd–lysine complex (392 nm), Pd–valine complex (391 nm) and lysine·HCl (0 nm), valine (0 nm), but the UV–vis spectra of Pd–lysine complex and Pd–valine complex were similar. Because Pd–valine and Pd–lysine complex were prepared at the same condition, and

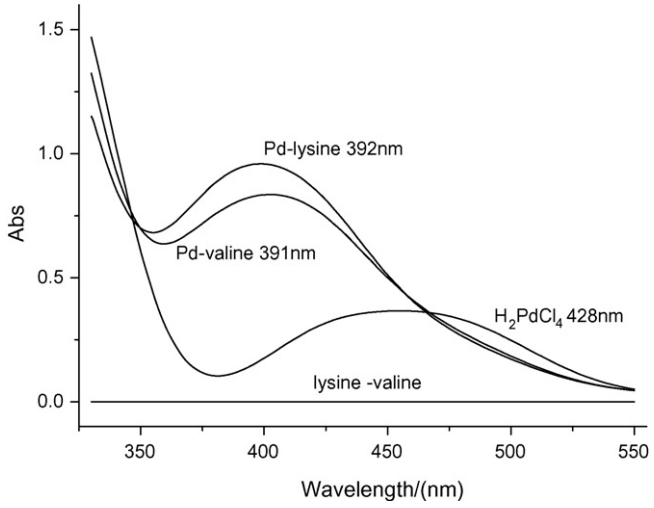

Fig. 11. The UV–vis spectra of Pd–aminoacid complexes and aminoacids.

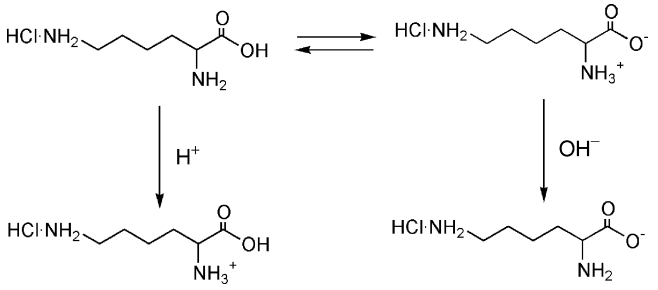

Scheme 1.

there are only α-NH_3^+ and –COO^- functional groups in valine, so the coordinate structures of Pd–valine and Pd–lysine complex were similar and the coordinate bonds were between Pd and α-NH_3^+ or –COO^- groups.

It is known that aminoacids undergo two reversible proton ionization steps (Scheme 1), therefore aminoacids may coordinate as the α-NH_2 and –COOH groups under certain condition.

3.2.3. The further confirmation of coordinate structure of Pd–lysine complex by IR, ^1H NMR spectra and single crystal diffraction determination

The IR absorbance peaks of valine and Pd–valine complex crystal were summarized in Table 1. The ascriptions of IR absorbance peaks were on the basis of Nakagawa et al. [19] and Ma et al. [20] suggests.

The IR absorbance peaks of –COO^- and –NH_3^+ groups of Pd–valine (1661 cm^{-1}, 1458 cm^{-1}; 1592 cm^{-1}, 1631 cm^{-1}) were different from that of valine (1561 cm^{-1}, 1416 cm^{-1}; 1627 cm^{-1}, 1503 cm^{-1}), the IR absorbance peaks of –COO^- group shifted from 1596 cm^{-1} to 1661 cm^{-1} and from 1416 cm^{-1} to 1458 cm^{-1}, the IR absorbance peak of –NH_3^+ group changed into two peaks and shifted from 1503 cm^{-1} to 1592 cm^{-1} and 1631 cm^{-1}, so the IR absorbance peaks of –COO^- and –NH_3^+ groups of valine took change after complex with H_2PdCl_4, they may interact with Pd atom. Because there are only –COO^- and α-NH_3^+ functional groups in valine, so α-NH_3^+ and –COO^- groups may interact with H_2PdCl_4 to form coordinate bonds. Because there were similar coordinate structure between Pd–valine complex and Pd–lysine complex (from Fig. 11), so α-NH_3^+ and –COO^- groups in lysine·HCl may form coordinate bonds with Pd atom. Because α-NH_3^+ cannot form the coordinate bond, the inter salt structure of valine and lysine·HCl must transfer into α-NH_2 carboxylic acid before coordination. Because the five-membered chelating ring structure was very stable, the coor-

Table 1
The parts of IR absorbance peaks and ascription of valine and Pd–valine complex crystal

Valine (cm^{-1})	Pd–valine (cm^{-1})	Ascription
1627		$\delta(NH_3^+)$
1596	1661	$\nu(COO^-)$
1503	1592, 1631	$\nu(NH_3^+)$
1473		$\delta(CH_3)$
1416	1458	$\nu(COO^-)$

dinate structure of Pd–lysine complex may be suggested as in Scheme 2.

The coordinate structure of Pd–lysine complex may be further verified by ^{1}H NMR spectra of Table 2, Fig. 12 and Scheme 3. After H_2PdCl_4 interacted with lysine·HCl, the signal corresponding to ^{1}H NMR peak of $–NH_3^+$ identified at δ 4.63 ppm changed into three signals, they were identified at δ 4.31 ppm, 4.58 ppm, 4.78 ppm, corresponding to ^{1}H NMR peaks of $–NH_2$, $–NH_3^+$, –COOH, respectively. The signal corresponding to ^{1}H NMR peak of –CH(2) shifted 0.1 ppm, from δ 3.53–3.57 ppm to δ 3.65–3.69 ppm, the other signals corresponding to ^{1}H NMR peaks of $–CH_2$(3–6) did not change, so the coordinate bonds were formed between α-NH_3^+ and $–COO^-$ groups and metal Pd. Because $–NH_3^+$ cannot form the coordinate bond, the inter salt of lysine·HCl must become α-NH_2 carboxylic acid before coordination.

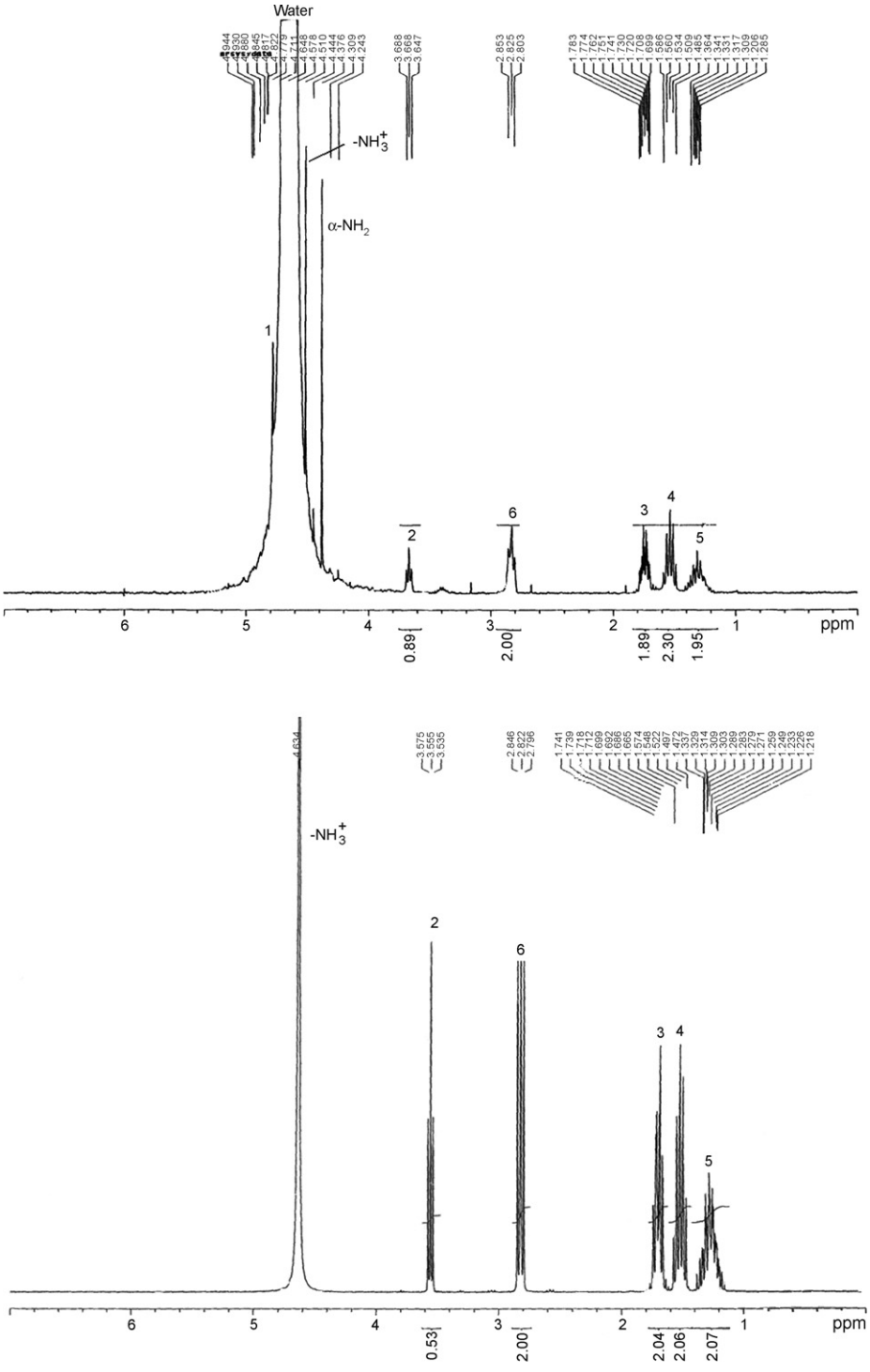

Fig. 12. ^{1}H NMR spectra of lysine·HCl and Pd–lysine complex.

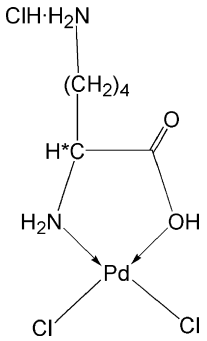

Scheme 2.

Table 2
The ^{1}H NMR spectra of lysine·HCl and Pd–lysine complex

Lysine·HCl, δ (ppm)	Pd–lysine, δ (ppm)	Ascription
1.22–1.32 (m, 2H)	1.28–1.36 (m, 2H)	CH_2(4)
1.47–1.55 (p, 2H)	1.50–1.58 (p, 2H)	CH_2(5)
1.66–1.74 (q, 2H)	1.69–1.78 (q, 2H)	CH_2(3)
2.79–2.85 (t, 2H)	2.80–2.85 (t, 2H)	CH_2(6)
3.53–3.57 (t, 1H)	3.65–3.69 (t, 1H)	CH(2)
4.63	4.31 (s, 2H)	NH_2
(s,	4.58 (s, 3H)	NH_3^+
6H)	4.78 (s, 1H)	COOH(1)

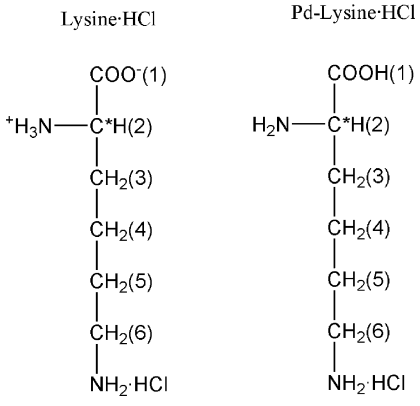

Scheme 3.

Under the same synthesis condition, Pd–lysine complex single crystal did not appear, but we obtained the single crystal of Pd–valine with the molecular formula of $[Pd(valine)_2]H_2O$. Crystal data for the complex, orthorhombic, space group $P2_12_12_1$, with $a = 9.627(2)$ Å, $b = 9.659(2)$ Å, $c = 15.278(4)$ Å, $V = 1420.7(5)$ Å^3, $Z = 4$, $R_1 = 0.0319$, $wR_2 = 0.0489$. The ORTEP drawing of the complex are shown in Fig. 13 and the selected bond lengths and angles are listed in Table 3. X-ray crystallography reveals α-NH_2 and –COO^- groups of each valine ligand coordinate to Pd to form one five-membered chelating ring. Since the Pd–valine complex contains two very stable five-membered chelating rings, it may not be suitable as catalyst.

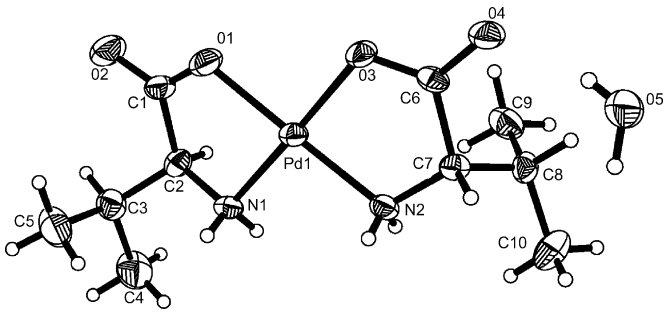

Fig. 13. The ORTEP view of $[Pd(valine)_2]·H_2O$.

Table 3
Selected bond lengths (Å) and bond angles (°) for $[Pd(valine)_2]·H_2O$

Bond distances (Å)	
Pd(1)–O(1)	1.990(3)
Pd(1)–N(2)	1.997(4)
Pd(1)–N(1)	2.001(4)
Pd(1)–O(3)	2.006(3)
Bond angles (°)	
O(1)–Pd(1)–N(2)	179.04(16)
O(1)–Pd(1)–N(1)	83.20(15)
N(2)–Pd(1)–N(1)	97.76(17)
O(1)–Pd(1)–O(3)	95.41(12)
N(2)-Pd(1)–O(3)	83.63(14)
N(1)–Pd(1)–O(3)	178.59(15)

3.3. The catalytic reactivity of Pd–lysine complex catalyst

3.3.1. Hydrogenation of p-chloronitrobenzene

Hydrogenation product distributions of *p*-chloronitrobenzene at different reaction conditions were summarized in Table 4, Pd–lysine complex catalyst may make *p*-chloronitrobenzene hydrogenate to *p*-chloroaniline in two-phases under mild reaction condition (50 °C, 0.1 MPa), the reaction conversion was 50.5% (GC) and the selectivity of *p*-chloroaniline was 98.0%. So the hydrogenation selectivity was good at lower pressure, little dechlorination reaction occurred. But at higher pressure, dechlorination product (aniline) increased, the aniline percent increased to 7.8%, the selectivity of *p*-chloroaniline was 90.6%, so Pd–lysine complex catalyst had dechlorination ability in two-phase reaction at higher pressure. When the reaction temperature raises to 75 °C, the conversion increased to 75.6%, but the aniline percent increased to 12.3%, the selectivity of *p*-chloroaniline decreased to 83.7%. When the catalyst amount increased one times, the conversion increased to 93.4%, but the selectivity was still 99.1%. Therefore, only the increase of catalyst amount could obtain good conversion and selectivity of *p*-chloroaniline.

Though there are four hydrogenation mechanistic pathways: (a) an oxidative addition of hydrogen, (b) hydride species, (c) unsaturated compound insertion (coordination), and (d) formation of an alkyl intermediate [21,22]. Pd–lysine complex prepared at pH 2.0–5.5 was complex catalyst, we suggest that the most possible hydrogenation mechanism should be hydride mechanism at pH 2.0–5.5. Because no other intermediate products were determined during reaction, many researches about the hydrogenation of –$ArNO_2$ have been published and the interme-

Table 4
Hydrogenation product distributions of *p*-chloronitrobenzene at different reaction conditions

T (°C)	Reaction condition		Product distribution (%)		Reaction conversion (%)	Selectivity of *p*-chloroaniline (%)
	H_2 pressure (MPa)	Catalyst amount (mL)	*p*-Chloroaniline	Aniline		
50	0.1	35	49.5	1.0	50.5	98.0
50	0.4	35	75.5	7.8	83.3	90.6
75	0.1	35	63.3	12.3	75.6	83.7
25	0.1	35	30.0	0.1	30.1	99.7
50	0.1	70	92.6	0.8	93.4	99.1
50	0.1	17.5	23.2	0.4	23.6	98.3

Catalyst concentration: 0.066 mmol/mL.

diate products have been identified, therefore, the hydrogenation reaction mechanism of $–NO_2$ in *p*-$ClArNO_2$ was suggested as in Scheme 4.

As there are two Cl^- coordinate bonds with Pd in Pd–lysine complex, the hydrogenation mechanism may be curtailed as Scheme 5. The $–ArNO_2$ may not be desorbed from the Pd complex until $–ArNH_2$ was formed because of alternating action of two Pd–H bonds. This action can make the hydrogenation rate increase.

There was dechlorination reaction during the hydrogenation reaction of *p*-$ClArNO_2$. The mechanism of hydrogenation dechlorination of *p*-$ClArNH_2$ was suggested in Scheme 6. Because the constitution of intermediate of five coordinate complex was difficult, the hydrogenation dechlorination rate was slower than $–ArNO_2$ hydrogenation.

After reaction, Pd–lysine complex catalyst may be recycled by simple phase separation. Because the water was produced during $–ArNO_2$ hydrogenation, the concentration of recycled Pd–lysine complex catalyst was diluted, thus the recycled Pd–lysine complex catalyst must be condensed under 80 °C before using again to obtain the same concentration catalyst. Under the same reaction condition, the recycled catalyst was used to catalyze the hydrogenation of *p*-$ClArNO_2$. After six recycling, the conversion and selectivity of *p*-$ClArNO_2$ changed less (Fig. 14), the UV–vis spectra of recycled catalysts were similar and same as the spectrum of the new catalyst (Fig. 15). Thus, the stability of Pd–lysine complex catalyst was good under the reaction condition (50 °C, 0.1 MPa, catalyst amount 35 mL, catalyst concentration 0.066 mmol/mL, the pH 4–4.5).

3.3.2. *Hydrogenation and dimerization of 2-nitro-5-chlorobenzotrifluoride*

According to GC–MS analysis and elemental analysis, we suggest when using ethanol as solvent and in H_2, after 2-nitro-5-chlorobenzotrifluoride was hydrogenated to 2-amino-5-chlorobenzotrifluride, the 2-amino-5-chlorobenzotrifluride may occur dimerization, the product was light yellow crystal. The crystal was washed by ethanol and dried in 80 °C, the total weight

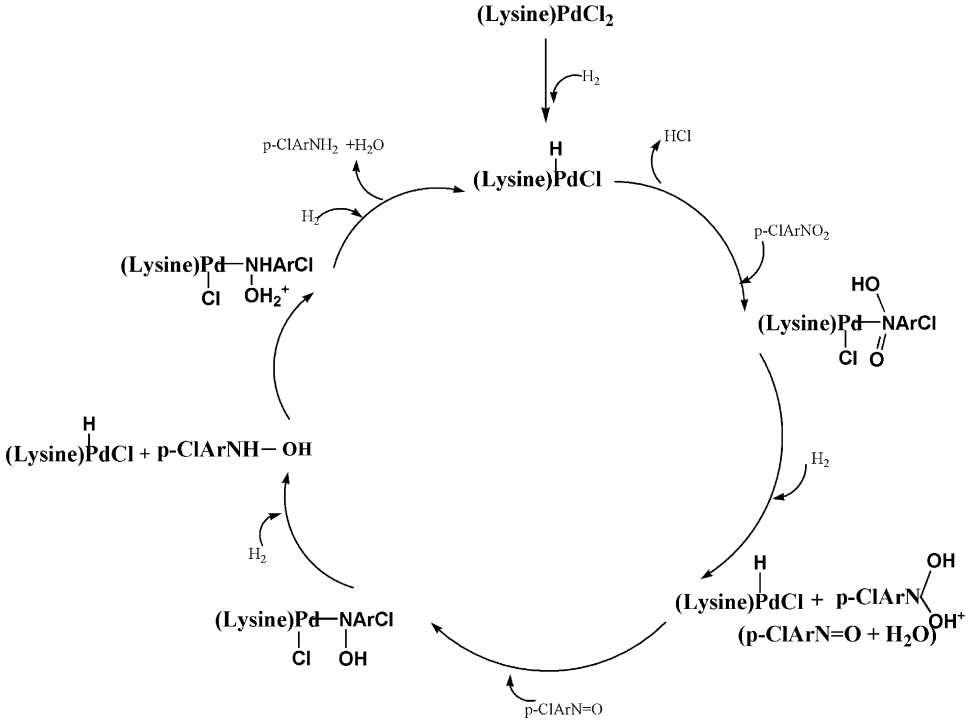

Scheme 4. Mechanism of hydride hydrogenation.

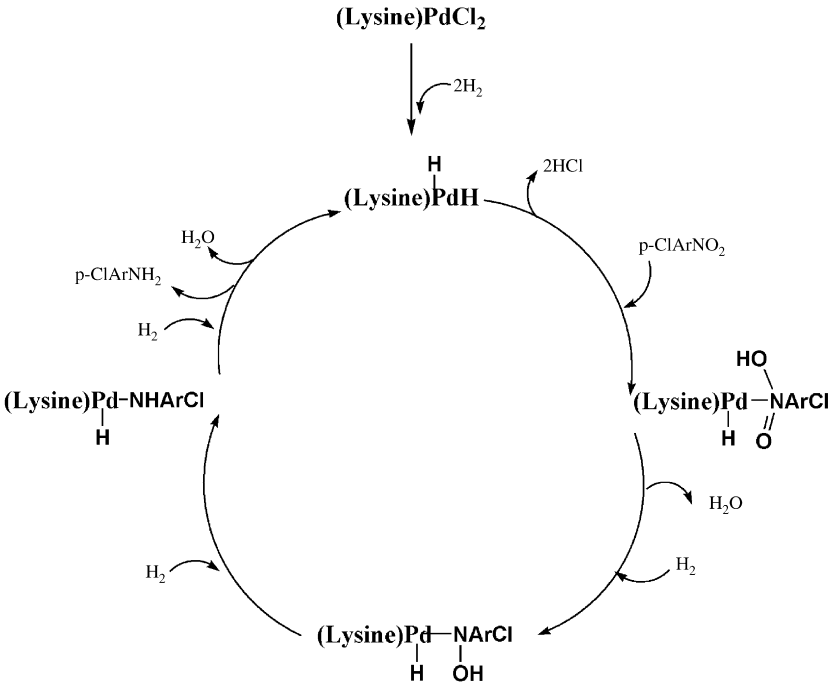

Scheme 5. Simple hydrogenation mechanism.

was 71.4 g, the conversion of 2-nitro-5-chlorobenzotrifluoride was 55%, the selectivity of dimmer was 98%. The reaction was as in Scheme 7.

Because polyaniline was produced at *o*- or *p*-position of amino group [23], the dimerization product was only at *o*-position of amino group.

According to above reaction results, the Pd–lysine complex prepared at pH 2–5.5 may be catalysts of hydrogenation of $-ArNO_2$, hydrogenation dechlorination of –ArCl and dimerization of $-ArNH_2$.

As the CH(2) in lysine is a chiral carbon atom, the Pd–lysine complex prepared above may be chiral catalyst. The enantios-

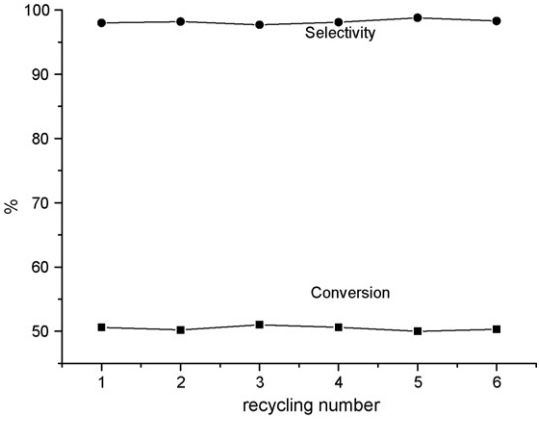

Fig. 14. The conversion and selectivity of six recycling reactions.

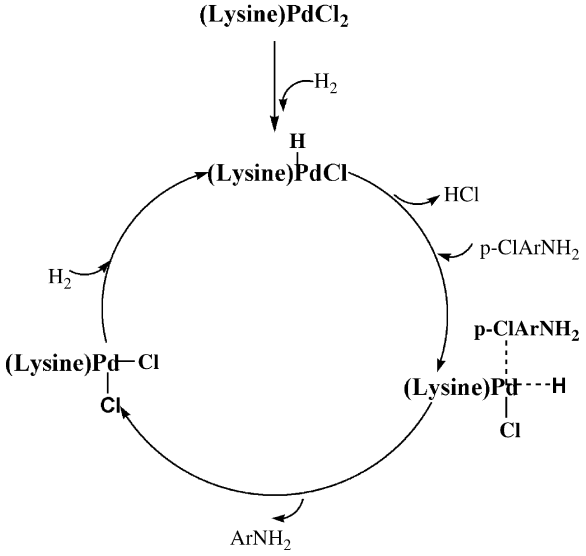

Scheme 6. Mechanism of hydrogenation dechorination.

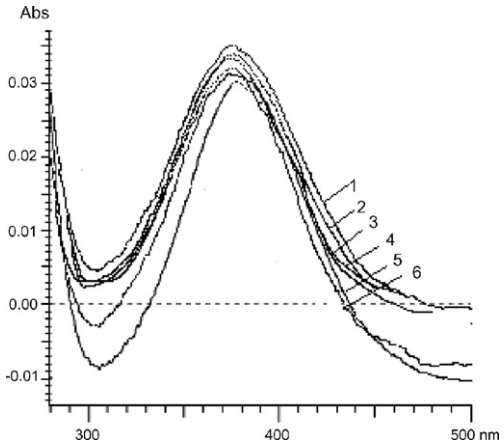

Fig. 15. The UV–vis spectra of the catalyst after six recycling reactions.

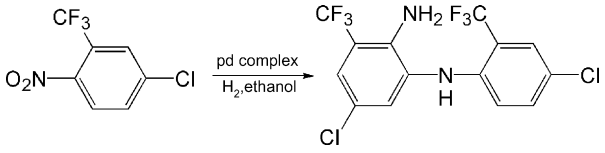

Scheme 7.

elective catalytic activity about these catalysts will be further researched.

4. Conclusion

Pd–lysine complex was prepared under mild condition and the N, O in α-NH_2 and –COOH groups may coordinate to the central Pd atom to form one stable five-membered chelating ring. The composition of Pd–lysine complex was [Pd(lysine·HCl)$(Cl)_2$] at pH 2–5.5, it may be used as two-phase hydrogenation catalyst for its property of water-soluble and it may easily be recycled by simple phase separation. Pd–lysine complex can make *p*-chloronitrobenzene hydrogenate to *p*-chloroaniline or hydrogenate and dechlorinate to aniline, and can make 2-nitro-5-chlorobenzotrifluoride hydrogenate and dimerize to dimer.

References

[1] W.A. Herrmann, C.W. Kohlpainter, Angew. Chem. Int. Ed. Engl. 32 (1993) 1524.
[2] P. Kalck, F. Monteil, Adv. Organomet. Chem. 34 (1992) 219.
[3] B. Cornils, E. Wiebus, Chemtech 33 (1995).
[4] B. Comils, E. Iebus, Chemtech 26 (1995) 33.
[5] J. Haggin, Chem. Eng. News 72 (1994) 28.
[6] K. Nomura, J. Mol. Catal. A 130 (1998) 1.
[7] I.T. Horvath (ed.), Catalysis in Water, J. Mol. Catal. A 116 (1997) (special issue).
[8] A.M. Tafesh, M. Beller, Tetrahedron Lett. 36 (1995) 9305.
[9] E. Monflier, S. Tilloy, G. Fremy, Y. Castanet, A. Mertreuxon, Tetrahedron Lett. 36 (1995) 9481.
[10] H. Jiang, Y. Xu, S.J. Liao, D.R. Yu, H. Chen, X.J. Li, J. Mol. Catal. A 130 (1998) 79.
[11] A.J. Gong, Q.H. Fan, Y.M. Chen, H.W. Liu, C.F. Chen, F. Xi, J. Mol. Catal. A 159 (2000) 225.
[12] J.M. Tour, J.P. Cooper, S.L. Pendalwar, J. Org. Chem. 55 (1990) 3452.
[13] J.M. Tour, S.L. Pendalwar, Tetrahedron Lett. 31 (1990) 4719.
[14] F. Joo, N. Balogh, L.I. Horvath, G. Filep, I. Horvath, L. Vigh, Anal. Biochem. 194 (1991) 34.
[15] M.T. Reeta, G. Lohmer, R. Schwicjard, Angew. Chem. Int. Ed. Engl. 36 (13/14) (1997) 1526.
[16] K. Kaneda, H. Kuwahara, T. Imanaka, J. Mol. Catal. 88 (1994) L267.
[17] Bruker AXS, SAINT Software Reference Manual, Bruker AXS, Madison, WI, 1998.
[18] G.M. Sheldrick, SHELXTL NT Version 5.1. Program for Solution and Refinement of Crystal Structures, University of Göttingen, Germany, 1997.
[19] I. Nakagawa, R.J. Hooper, J.L. Walter, Spectrachonica Acta 21 (1965) 1.
[20] A.Z. Ma, L.M. Li, S.Q. Xi, Chin. J. Appl. Chem. 12 (1995) 48.
[21] E.W. Stern, P.K. Maples, J. Catal. 27 (1972) 120.
[22] D. Foster, J.F. Roth (Eds.), Homogeneous Catalysis. Part II. Advanced Chemical Series, 1974, p. 132.
[23] Y. Cao, A. Andreatta, A.J. Heeger, P. Smith, Polymer 30 (1989) 230.